

1 **A global hydrothermal reactor triggered prebiotic synthesis on Earth**

2 Chiara Boschi¹, Andrea Dini^{1,*}, Gretchen L. Früh-Green², Luca Caricchi³

3 1) Institute of Geosciences and Earth Resources – CNR, Via G. Moruzzi 1, 56124 Pisa, Italy

4 2) Department of Earth Sciences, ETH, Sonneggstrasse 5, 8092 Zurich, Switzerland

5 3) Department of Earth Sciences, University of Geneva, rue des Maraîchers 13, 1205, Geneva, Switzerland

6

7 *Corresponding author: andrea.dini@igg.cnr.it

8

9 **Biosignatures in the rock record limit the time available for life to start on Earth to 600-**
10 **800 million years¹ (4.5-3.7 Ga; Hadean-Archean). Whether the conditions for the**
11 **synthesis of complex organic molecules were unique to this time or remain present today**
12 **is unclear, but understanding these conditions is essential for the search of life on other**
13 **planets. The outer portion of the Hadean Earth consisted of a thick mafic crust² and the**
14 **upper mantle from which the crust was extracted³. Here we show that the recycling of**
15 **the Earth's initial crust to produce the first continental crust^{2,4-6}, resulted in extreme**
16 **thinning of the initial mafic crust allowing the interaction between ocean water and the**
17 **upper mantle at a global scale. This global hydrothermal reactor was similar to the**
18 **present-day active “Lost City Hydrothermal Field”⁷, but extended on a planetary scale.**
19 **The geological record indicates that the interaction between H₂O and olivine-rich rocks**
20 **resulted in the production of 5-20 vol.% brucite⁸⁻¹⁰, a key catalytic mineral for high**
21 **temperature stabilisation, selection and phosphorylation of ribose^{11,12}. The secular**
22 **cooling of our planet², the accretion of continental crust, and deposition of sediments**
23 **progressively shut down the global reactor. These processes dramatically reduced the**
24 **production of brucite and the probability of synthesizing prebiotic molecules. Our results**
25 **suggest that the geodynamic evolution of planets should be considered when searching**
26 **for life in the Universe.**

27 The period during which life originated on Earth is limited by the onset of habitability and the
28 appearance of the first documented lifeforms¹. In the most favourable scenario, the Earth could
29 have been habitable as early as 4.5-4.3 Ga (Refs.^{3,13}). The first lifeforms are described in the
30 geological record at 3.7 Ga (Ref.¹⁴), which implies that pre-biotic molecules (PBM) must have
31 been available and possibly abundant in this 600–800 million year time-window. Discounting
32 an external input of life by asteroids, hydrothermal systems in an oceanic environment^{7,15} or
33 on continents, driven by magmatic activity¹⁶ or by natural nuclear reactors¹⁷, are potential
34 niches for the synthesis of PBM. These systems provide the ingredients for the synthesis of the
35 building blocks of life in the early Earth: liquid water (oceans or continental pools), a variety
36 of gases (atmosphere and degassing) and minerals acting as catalysers¹⁸.

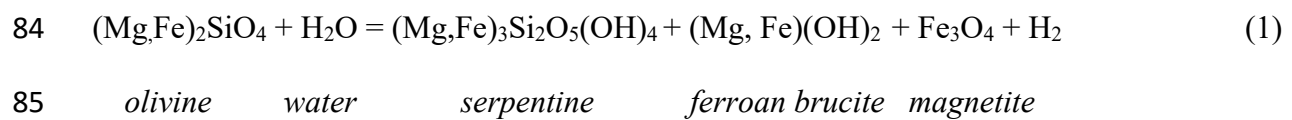
37 The discovery of submarine hydrothermal vents around Galapagos¹⁹ lead to the first hypothesis
38 for the synthesis of PBM in high-temperature mafic-hosted hydrothermal systems¹⁵. This idea
39 was later transferred to the low-temperature Lost City Hydrothermal Field (LCHF), an
40 ultramafic-hosted alkaline hydrothermal system discovered in 2000 near the slow-spreading
41 Mid-Atlantic Ridge⁷ (Fig. 1). Low temperature (~100 °C) as well as reduced and alkaline
42 conditions^{7,20} are essential for the formose reaction, and have removed some of the theoretical
43 obstacles for a hydrothermal origin of life. Moreover, the production of a significant amount
44 of H₂ and CH₄ and formate vital for supporting life, were considered a significant improvement
45 with respect to the hypothesis of Ref.¹⁵. However, the formation of the building blocks of life
46 is *per se* insufficient and any hypothesis for the synthesis of PBM should include selection,
47 stabilization and phosphorylation of ribose in a natural environment²¹.

48 Here, instead of starting from a defined set of chemical reactions, we take a different approach
49 and assess which environments are potentially capable of synthesising PBM²² in the presence
50 of well-known catalytic minerals¹⁸, were available in the early Earth. We consider that the
51 probability of synthesizing PBM increases with the proportion of the planet in which all the

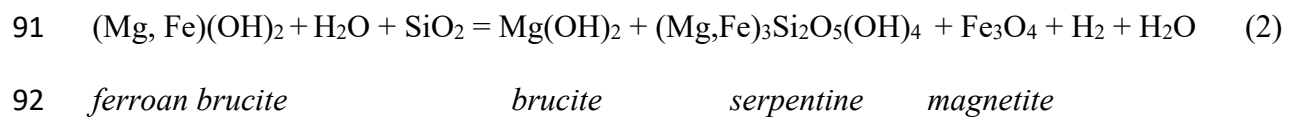
52 essential requirements are met. Natural nuclear reactors would be punctual features as they
53 require high-grade U ore deposits that are unlikely to be abundant in a chemically
54 undifferentiated Hadean crust²³. Continental hydrothermal systems are also punctual features
55 as the supply of heat is associated with volcanic systems and distributed along belts in a
56 discontinuous fashion. Hydrothermal systems associated with mid-ocean ridges occur along
57 linear features. Thus, all these environments would be active on a rather limited portion of the
58 planet. Looking back to the early Earth, after Theia's impact and the formation of the Moon at
59 about 4.51 Ga (Ref.²⁴), a magma ocean was established that cooled and degassed¹³ to produce
60 the early atmosphere in a few million years¹³. Gravitational instability of the outermost portion
61 of the solidified magma ocean (50 vol.% olivine, 25 vol. % cpx, 20 vol.% opx, 5 vol.% plg)
62 eventually resulted in its wholesale or incremental removal¹³ accommodated by mantle ascent,
63 its partial melting and the construction of a thick (20-40 km) crust². The high degree of partial
64 melting that formed this initial crust left a residual, olivine-rich upper mantle². The geological
65 investigation of Archean terrains suggest that the initial mafic/ultramafic crust was recycled
66 into the mantle². During recycling, the hydrated mafic/ultramafic crust would partially melt
67 and a 10-30% (Ref.²⁵) fraction of the removed material would have resurfaced as the early
68 continental crust (Tonalite-Trondhjemite-Granodiorite; TTG)^{6,26,27}. The newly formed crust
69 was a fraction of the recycled mafic crust and the ocean floor must have been covered by much
70 less sediments than today²⁸. Thus, during this period of crustal regeneration, the potential
71 exposure and interaction between the depleted upper mantle with water would have been more
72 significant than at present. This, in turn, would have increased the potential for systems similar
73 to the LCHF to develop^{7,20}.

74 At LCHF, the hydrothermal modification of the ultramafic mantle produces mainly serpentine
75 and magnetite and, where alkaline hydrothermal fluids discharged into the ocean, additional
76 brucite and carbonate (Fig. 1). These hydrothermal systems (LCHF, as well as hybrid

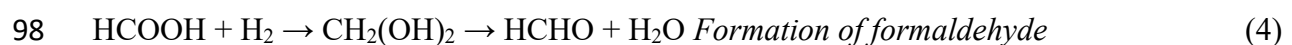
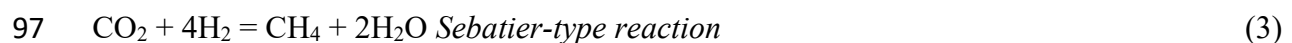
77 Logatchev and Rainbow systems^{29,30}) are extremely dynamic. Multistage serpentinization
 78 generate a wide variety of niches characterised by specific pH, redox potential, temperatures,
 79 and activities of elements critical for prebiotic synthesis, distributed in space and changing with
 80 time^{8-10,29,31-36}. Moreover, abiotic hydrocarbons and carboxylic acids have been described in
 81 hydrothermally altered mantle rocks of LCHF³⁷. The following are some of the fundamental
 82 reactions occurring in hydrothermal systems hosted by mantle lithologies^{31,38}. The
 83 serpentinization of olivine produces ferroan brucite, serpentine, and magnetite^{9,39}:



86 The formation of hydrogen is related to the amount of ferric iron in serpentine and to the moles
 87 of magnetite produced (Eq. 1)^{10,31,38}. Eventual increase in temperature (e.g. magma injection)
 88 or changes in other thermodynamic variables (e.g. oxygen fugacity) destabilises ferroan brucite
 89 leading to the massive precipitation of magnetite, associated with abundant production of
 90 hydrogen:



93 Fundamentally, the reaction between H₂ produced by hydrothermal circulation in ultramafic
 94 rocks, and CO₂ released from the mantle or magma degassing, produces CH₄ as a final product
 95 with methanediol as an intermediate reaction product (Eq. 3). The reaction of methanediol and
 96 H₂, produces formaldehyde (Eq. 4), the building block of life:



99 Starting with formaldehyde and glycolaldehyde, under alkaline conditions and in the presence
 100 of cation catalysts like Mg²⁺ and Ca²⁺, the formose reaction produces a variety of pentoses
 101 (ribose, arabinose, xylose, lyxose, ribulose, xylulose⁴⁰). Ribose, the essential constituent of

102 RNA and DNA, is the least stable of the pentoses and rapidly decomposes to generate
103 polymeric tar mixtures¹¹. Selection, stabilization and accumulation of ribose, and its
104 phosphorylation to form RNA units, are key factors to unravel prebiotic chemistry and the
105 origin of life⁴¹. Borates and boric acid have been experimentally demonstrated to have this
106 stabilizing effect on pentoses and to select ribose^{42,43}. Moreover, phosphorus is necessary for
107 phosphorylation, which is also assisted by borates and boric acid⁴⁴. Because of the important
108 role of borates, various authors have proposed different models for the accumulation of large
109 quantities of these minerals⁴⁵, which requires differentiated and evolved continental crust and
110 subaerial ponds undergoing desiccation. The presence of such regions with high concentrations
111 of B and P cannot be determined with any certainty as almost all of the Hadean rock record
112 simply does not exist. Here we propose that prebiotic chemistry did not take place in borate
113 deposits enriched in P but was mediated by the key catalyser brucite. This mineral adsorbs
114 large quantities of B and P (Refs.^{11,46-48}), while being stable in an environment characterised
115 by high and variable pH, a range of redox conditions, and participates in the synthesis of
116 formaldehyde. Additionally, the reactions involving ferroan brucite and brucite modulate the
117 release of H₂ and the availability of Mg²⁺. These elements and conditions are all required to
118 select ribose from the other pentoses, stabilise it to relatively high temperatures and facilitate
119 phosphorylation which is key for the transition to self-replicating macro-molecules^{11,48} (Eq. 2).
120 While other potential catalysers could have been stabilised by the interaction between mafic
121 crust and ocean water, their abundance would have been extremely limited with respect to the
122 amount of brucite produced by interaction between water and mantle lithologies (Fig. 2). This
123 is especially true for the olivine-rich mantle produced by high degrees of melting during the
124 production of the early mafic crust.

125 We propose that during the period of crust regeneration in the Hadean-Archean, a global
126 ultramafic reactor was active, producing copious amounts of brucite and thus PBM.

127 Fundamental for the plausibility of a global ultramafic reactor is the assumption that the
128 oceanic crust was sufficiently thin to allow oceanic water to penetrate into the upper mantle
129 and trigger the formation of brucite. To estimate the evolution of crustal thickness in time, once
130 clement conditions were established on Earth (4.5-4.3 Ga; Refs.^{13,49}), we performed mass
131 balance calculations using a Monte Carlo approach (100'000 repetitions). We rely on
132 geological^{2,50} and experimental petrological²⁵ constraints to define a plausible range of the
133 parameters (Methods). The results show that due to recycling the Hadean crust progressively
134 thins and for the largest number of simulations, reaches a minimum after around 200-300 Myrs
135 from the onset of Hadean crust recycling (Fig. 3b; Note that for simplicity of comparison in
136 the calculations we have always assumed that recycling started at 4.51 Ga). At this time the
137 thickness of the mafic crust obtained from the largest number of simulations is lower than 2000
138 m, which is significantly thinner than today's average oceanic crust (6000 m; Ref.³⁰; Fig. 3c).
139 This is in agreement with the decreasing thickness of the oceanic crust observed when large
140 portions of the Earth crust disaggregate increasing the cooling rate of the mantle⁵¹. It should be
141 noted that because we do not consider recycling of newly formed mafic and TTG-type crust,
142 all thicknesses presented are maximum estimates. Additionally, the rate of production of new
143 crust was likely heterogeneous, as also shown by numerical modelling^{4,5}. Thus, our mass
144 balance suggests that at around 4.5-4 Ga, large portions of the upper mantle were either covered
145 by a thin oceanic crust or exposed on the ocean floor. This would have allowed the interaction
146 between ocean water and the upper mantle⁵² at a global scale, triggering the production of
147 substantial amounts of brucite both above and below sea level (Fig. 1) and boosting the
148 production of PBM. As these conditions were never reproduced on Earth, any process that
149 would have isolated the mantle from the interaction with water within this optimal time window
150 might have left the Earth a lifeless planet. At present, the upper mantle is exposed to the
151 interaction with water only in very limited portions of our planet (0.29% of the surface;

152 Methods). Hence, the probability of today's Earth to synthesis PBM is vanishingly small in
153 comparison to the Hadean-Archean. As a result of the intimate relationship between life and
154 the evolution of planets, the rate and sequence of geological processes, as well as the presence
155 of catalytic minerals should be considered when searching for life in the Universe.

156

157 **Methods**

158 We consider that the recycling of the mafic/ultramafic crust Hadean Earth's crust results in the
159 production of TTGs^{2,6,53}. We make no inference on the actual geodynamic process responsible
160 for crustal recycling. We consider that the degree of partial melting of a mafic/ultramafic
161 protolith required to produce TTGs varies between 0.1 and 0.3 (*mf*; Ref.²⁵). Estimates for the
162 initial thickness of the mafic/ultramafic crust in the Hadean (Th_{iH}) vary between 20 and 40 km
163 as inferred from non-arc basalts and cratonic peridotite residues². Thus, we selected this range
164 for our calculations. We consider to end member scenarios for the growth of the mass of
165 continental crust over time ($M_c(t)$) from Ref.⁵⁴ (Fig. 3a):

$$166 \quad M_c(t) = \frac{M_c(t_p)}{1 - e^{-k_g(t_p - t_s)}} (1 - e^{-k_g(t - t_s)}) \quad (1)$$

167 Where $M_c(t_p)$ is the current mass of continental crust, t_s and t_p correspond to time at the onset
168 of growth of continental crust and the present time measured from the beginning of the solar
169 system, respectively, k_g is a growth constant and t is time. Considering a radius of the Earth of
170 6371 km and a density of the continental crust (ρ_{cc}) of 2700 kg/m³, we can convert $M_c(t)$ into
171 the evolution of continental crust thickness (Th_{cc}) over time and perform our mass balance
172 calculations in 1D. We assume a density of the mafic/ultramafic Hadean crust of 2900 kg/m³
173 (ρ_H ; different densities do not affect significantly our calculations) and calculate the temporal
174 evolution of the thickness of the mafic/ultramafic crust (Th_H , which is recycled to produce
175 continental crust) as:

176 $Th_H = Th_{iH} - \frac{Th_{cc} \rho_{cc}}{mf \rho_H}$ (2)

177 Additionally, we consider that while Hadean mafic and ultramafic crust was recycled to
 178 produce continental crust, the partial melting of the mantle also produced also new mafic crust.
 179 To estimate the thickness of new mafic crust (Th_m) we use the Archean geological record. The
 180 fraction of volcanic rocks in Greenstone belts (fv_{Gb}) varies between 0.2 and 0.8, of which a
 181 fraction of 0.5 to 0.9 is represented by mafic rocks² (f_m). We consider that the same proportions
 182 also apply to intrusive rocks (intrusive mafic=gabbros; fi_g), but the repartition does not change
 183 the results of our calculations. The thickness of mafic rocks is:

184 $Th_m = Th_{cc}fv_{Gb}f_m + Th_{cc}(1 - fv_{Gb})fi_g$ (3)

185 To compare the amount of upper mantle rocks potentially interacting with seawater in the
 186 Hadean and nowadays, we estimate the mantle presently exposed on the seafloor. Mantle-
 187 derived ultramafic rocks occur along the axial valley of slow spreading ridges (spreading rates
 188 <4 cm/yr), most commonly near axial discontinuities. Ref.³³ estimated that mantle lithologies
 189 represent about 23% of the newly formed oceanic crust along slow spreading ridges. Moving
 190 off-axis (>100 km), the oceanic crust is rapidly blanketed by sediments²⁸ hampering the
 191 interaction between seawater and mantle rocks. Considering the total length of slow spreading
 192 ridges (31880 km), 100 km distance on each side of the ridge, and the percentage of mantle
 193 rocks exposed at the seafloor (23%), the ultramafic reactive surface represents 0.29% of the
 194 total Earth's surface.

195

196 **References**

- 197 1. Pearce, B. K. D., Tupper, A. S., Pudritz, R. E. & Higgs, P. G. Constraining the Time Interval for the
 198 Origin of Life on Earth. *Astrobiology* **18**, 343–364 (2018).
- 199 2. Herzberg, C. & Rudnick, R. Formation of cratonic lithosphere: An integrated thermal and petrological
 200 model. *Lithos* **149**, 4–15 (2012).
- 201 3. O'Neill, C. & Debaille, V. The evolution of Hadean–Eoarchean geodynamics. *Earth Planet. Sci. Lett.*

- 202 406, 49–58 (2014).
- 203 4. Sizova, E., Gerya, T., Stüwe, K. & Brown, M. Generation of felsic crust in the Archean: A geodynamic
204 modeling perspective. *Precambrian Res.* **271**, 198–224 (2015).
- 205 5. Capitanio, F. A., Nebel, O., Cawood, P. A., Weinberg, R. F. & Chowdhury, P. Reconciling thermal
206 regimes and tectonics of the early Earth. *Geology* **47**, 923–927 (2019).
- 207 6. Moyen, J.-F. & Martin, H. Forty years of TTG research. *Lithos* **148**, 312–336 (2012).
- 208 7. Kelley, D. S. *et al.* An off-axis hydrothermal vent field near the Mid-Atlantic Ridge at 30° N. *Nature*
209 **412**, 145–149 (2001).
- 210 8. Templeton, A. S. & Ellison, E. T. Formation and loss of metastable brucite: does Fe(II)-bearing brucite
211 support microbial activity in serpentinizing ecosystems? *Philos. Trans. R. Soc. A Math. Phys. Eng. Sci.*
212 **378**, 20180423 (2020).
- 213 9. Boschi, C. *et al.* Brucite-driven CO₂ uptake in serpentinized dunites (Ligurian Ophiolites,
214 Montecastelli, Tuscany). *Lithos* **288–289**, 264–281 (2017).
- 215 10. Klein, F., Humphris, S. E. & Bach, W. Brucite formation and dissolution in oceanic serpentinite.
216 *Geochemical Perspect. Lett.* 1–5 (2020). doi:10.7185/geochemlet.2035
- 217 11. Holm, N. G., Dumont, M., Ivarsson, M. & Konn, C. Alkaline fluid circulation in ultramafic rocks and
218 formation of nucleotide constituents: a hypothesis. *Geochem. Trans.* **7**, 7 (2006).
- 219 12. Estrada, C. F. *et al.* Aspartate transformation at 200 °C with brucite [Mg(OH)₂], NH₃, and H₂:
220 Implications for prebiotic molecules in hydrothermal systems. *Chem. Geol.* **457**, 162–172 (2017).
- 221 13. Elkins-Tanton, L. T. Linked magma ocean solidification and atmospheric growth for Earth and Mars.
222 *Earth Planet. Sci. Lett.* **271**, 181–191 (2008).
- 223 14. Dodd, M. S. *et al.* Evidence for early life in Earth’s oldest hydrothermal vent precipitates. *Nature* **543**,
224 60–64 (2017).
- 225 15. Corliss, J. B., Baross, J. A. & Hoffman, S. E. An hypothesis concerning the relationship between
226 submarine hot springs and the origin of life on earth. *Oceanol. Acta* **1980**, 59–69 (1981).
- 227 16. Mulkidjanian, A. Y., Bychkov, A. Y., Dibrova, D. V., Galperin, M. Y. & Koonin, E. V. Open Questions
228 on the Origin of Life at Anoxic Geothermal Fields. *Orig. Life Evol. Biosph.* **42**, 507–516 (2012).
- 229 17. Ebisuzaki, T. & Maruyama, S. Nuclear geyser model of the origin of life: Driving force to promote the
230 synthesis of building blocks of life. *Geosci. Front.* **8**, 275–298 (2017).
- 231 18. Hazen, R. M. Chance, necessity and the origins of life: a physical sciences perspective. *Philos. Trans. R.*

- 232 *Soc. A Math. Phys. Eng. Sci.* **375**, 20160353 (2017).
- 233 19. Corliss, J. B. *et al.* Submarine Thermal Springs on the Galápagos Rift. *Science (80-.)*. **203**, 1073–1083
234 (1979).
- 235 20. Früh-Green, G. L. *et al.* 30,000 Years of Hydrothermal Vent Field. *Science (80-.)*. **301**, 495–498
236 (2003).
- 237 21. Sasselov, D. D., Grotzinger, J. P. & Sutherland, J. D. The origin of life as a planetary phenomenon. *Sci.*
238 *Adv.* **6**, 1–10 (2020).
- 239 22. Lang, S. Q. & Brazelton, W. J. Habitability of the marine serpentinite subsurface: a case study of the
240 Lost City hydrothermal field. *Philos. Trans. R. Soc. A Math. Phys. Eng. Sci.* **378**, 20180429 (2020).
- 241 23. Smit, M. A. & Mezger, K. Earth's early O₂ cycle suppressed by primitive continents. *Nat. Geosci.* **10**,
242 788–792 (2017).
- 243 24. Barboni, M. *et al.* Early formation of the Moon 4.51 billion years ago. *Sci. Adv.* **3**, 1–9 (2017).
- 244 25. Moyaen, J.-F. & Stevens, G. Experimental constraints on TTG petrogenesis: Implications for Archean
245 geodynamics. in *Geophysical Monograph Series* **164**, 149–175 (2006).
- 246 26. Dhuime, B., Wuestefeld, A. & Hawkesworth, C. J. Emergence of modern continental crust about 3
247 billion years ago. *Nat. Geosci.* **8**, 552–555 (2015).
- 248 27. Korenaga, J. Estimating the formation age distribution of continental crust by unmixing zircon ages.
249 *Earth Planet. Sci. Lett.* **482**, 388–395 (2018).
- 250 28. Ewing, M., Carpenter, G., Windisch, C. & Ewin, J. Sediment Distribution in the Oceans: The Atlantic.
251 *Geol. Soc. Am. Bull.* **84**, 71 (1973).
- 252 29. Charlou, J. L. *et al.* High production and fluxes of H₂ and CH₄ and evidence of abiotic hydrocarbon
253 synthesis by serpentinization in ultramafic-hosted hydrothermal systems on the Mid-Atlantic Ridge. in
254 *Diversity of Hydrothermal Systems on Slow Spreading Ocean Ridges* 265–296 (2010).
255 doi:10.1029/2008GM000752
- 256 30. Staudigel, H. Hydrothermal Alteration Processes in the Oceanic Crust. in *Treatise on geochemistry*
257 (2003).
- 258 31. Bach, W., Garrido, C. J., Paulick, H., Harvey, J. & Rosner, M. Seawater-peridotite interactions: First
259 insights from ODP Leg 209, MAR 15°N. *Geochemistry, Geophys. Geosystems* **5**, n/a-n/a (2004).
- 260 32. Boschi, C., Dini, A., Früh-Green, G. L. & Kelley, D. S. Isotopic and element exchange during
261 serpentinization and metasomatism at the Atlantis Massif (MAR 30°N): Insights from B and Sr isotope

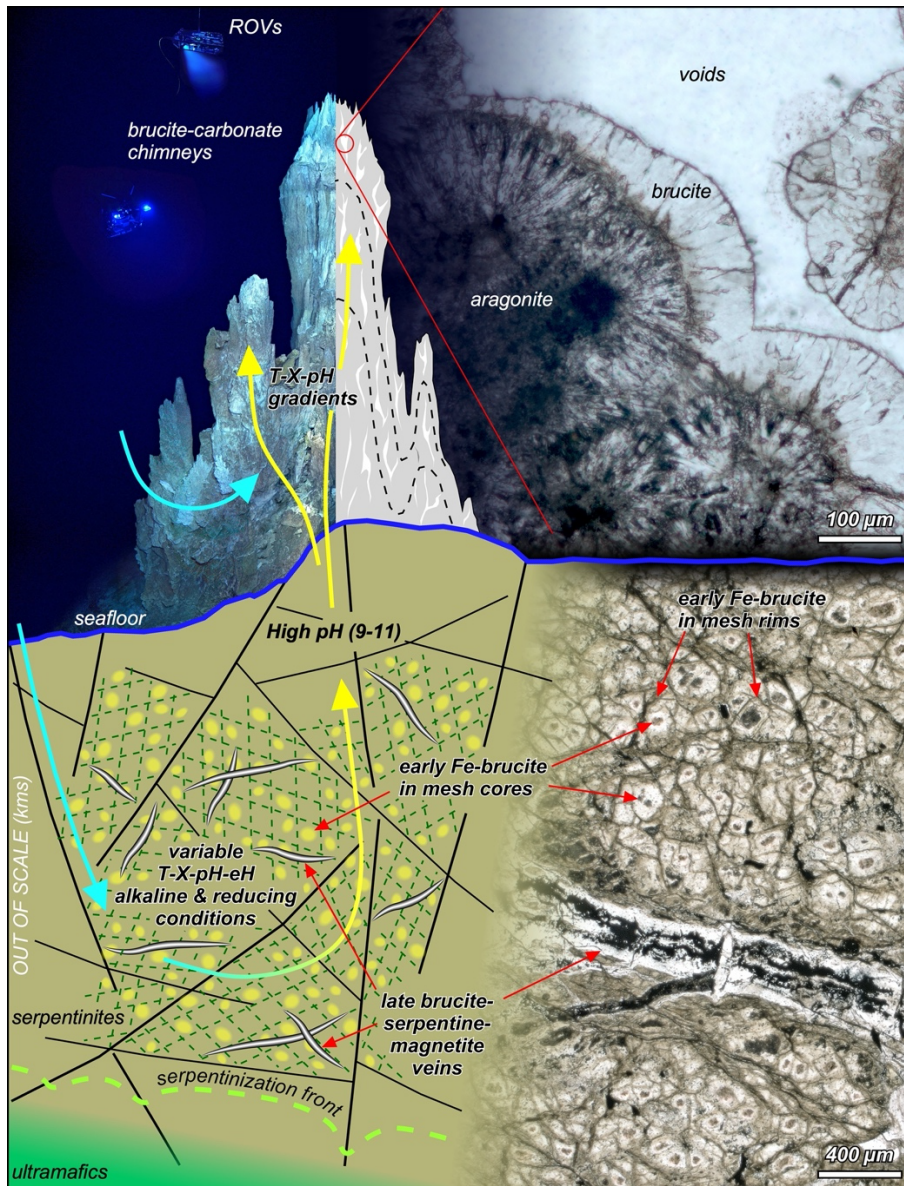
- 262 data. *Geochim. Cosmochim. Acta* **72**, 1801–1823 (2008).
- 263 33. Cannat, M., Fontaine, F. & Escartín, J. Serpentinization and associated hydrogen and methane fluxes at
264 slow spreading ridges. in *Diversity of Hydrothermal Systems on Slow Spreading Ocean Ridges* 241–264
265 (2010). doi:10.1029/2008GM000760
- 266 34. Malvoisin, B. Mass transfer in the oceanic lithosphere: Serpentinization is not isochemical. *Earth*
267 *Planet. Sci. Lett.* **430**, 75–85 (2015).
- 268 35. Bach, W., Peucker-Ehrenbrink, B., Hart, S. R. & Blusztajn, J. S. Geochemistry of hydrothermally
269 altered oceanic crust: DSDP/ODP Hole 504B - Implications for seawater-crust exchange budgets and
270 Sr- and Pb-isotopic evolution of the mantle. *Geochemistry, Geophys. Geosystems* **4**, 40–55 (2003).
- 271 36. Hildebrand, R. S., Hoffman, P. F., Housh, T. & Bowring, S. A. The nature of volcano-plutonic relations
272 and the shapes of epizonal plutons of continental arcs as revealed in the Great Bear magmatic zone,
273 northwestern Canada. *Geosphere* **6**, 812–839 (2010).
- 274 37. Ménez, B. *et al.* Abiotic synthesis of amino acids in the recesses of the oceanic lithosphere. *Nature* **564**,
275 59–63 (2018).
- 276 38. Evans, B. W. Lizardite versus antigorite serpentinite: Magnetite, hydrogen, and life(?). *Geology* **38**,
277 879–882 (2010).
- 278 39. Boschi, C., Früh-Green, G. L., Delacour, A., Karson, J. A. & Kelley, D. S. Mass transfer and fluid flow
279 during detachment faulting and development of an oceanic core complex, Atlantis Massif (MAR 30°N).
280 *Geochemistry, Geophys. Geosystems* **7**, n/a-n/a (2006).
- 281 40. Joyce, G. F. RNA evolution and the origins of life. *Nature* **338**, 217–224 (1989).
- 282 41. Scorei, R. Is Boron a Prebiotic Element? A Mini-review of the Essentiality of Boron for the Appearance
283 of Life on Earth. *Orig. Life Evol. Biosph.* **42**, 3–17 (2012).
- 284 42. Furukawa, Y., Horiuchi, M. & Kakegawa, T. Selective Stabilization of Ribose by Borate. *Orig. Life*
285 *Evol. Biosph.* **43**, 353–361 (2013).
- 286 43. Ricardo, A. Borate Minerals Stabilize Ribose. *Science (80-.)*. **303**, 196–196 (2004).
- 287 44. Furukawa, Y. & Kakegawa, T. Borate and the Origin of RNA: A Model for the Precursors to Life.
288 *Elements* **13**, 261–265 (2017).
- 289 45. Grew, E. S., Bada, J. L. & Hazen, R. M. Borate Minerals and Origin of the RNA World. *Orig. Life Evol.*
290 *Biosph.* **41**, 307–316 (2011).
- 291 46. Xiao, J., Xiao, Y. K., Liu, C. Q. & Jin, Z. D. Boron isotope fractionation during brucite deposition from

- 292 artificial seawater. *Clim. Past* **7**, 693–706 (2011).
- 293 47. Prodromou, K. P. Boron adsorption on freshly prepared Mg(OH)₂. *Neues Jahrb. für Mineral. -*
294 *Monatshefte* **2004**, 221–227 (2004).
- 295 48. Karl, D. M. & Tien, G. MAGIC: A sensitive and precise method for measuring dissolved phosphorus in
296 aquatic environments. *Limnol. Oceanogr.* **37**, 105–116 (1992).
- 297 49. Sleep, N. H. Geological and Geochemical Constraints on the Origin and Evolution of Life. *Astrobiology*
298 **18**, 1199–1219 (2018).
- 299 50. Taylor, S. R. & McLennan, S. M. *The continental crust: its composition and evolution*. (Blackwell
300 Scientific Publications, 1985).
- 301 51. Van Avendonk, H. J. A., Davis, J. K., Harding, J. L. & Lawver, L. A. Decrease in oceanic crustal
302 thickness since the breakup of Pangaea. *Nat. Geosci.* **10**, 58–61 (2017).
- 303 52. Zwan, F. M., Chadwick, J. P. & Troll, V. R. Textural history of recent basaltic-andesites and plutonic
304 inclusions from Merapi volcano. *Contrib. to Mineral. Petrol.* **166**, 43–63 (2013).
- 305 53. Sizova, E., Gerya, T., BROWN, M. & Perchuk, L. L. ScienceDirect.com - Lithos - Subduction styles in
306 the Precambrian: Insight from numerical experiments. *LITHOS* (2010).
- 307 54. Rosas, J. C. & Korenaga, J. Rapid crustal growth and efficient crustal recycling in the early Earth:
308 Implications for Hadean and Archean geodynamics. *Earth Planet. Sci. Lett.* **494**, 42–49 (2018).
- 309 55. Alt, C., Honnorez, J., Laverne, C. & Emmermann, R. Hydrothermal alteration of a 1 km section through
310 the upper oceanic crust. DSDP Hole 504B: Mineralogy, chemistry and evolution of seawater-basalt
311 interactions. *J. Geophys.* **91**, 309–335 (1986).

312

313

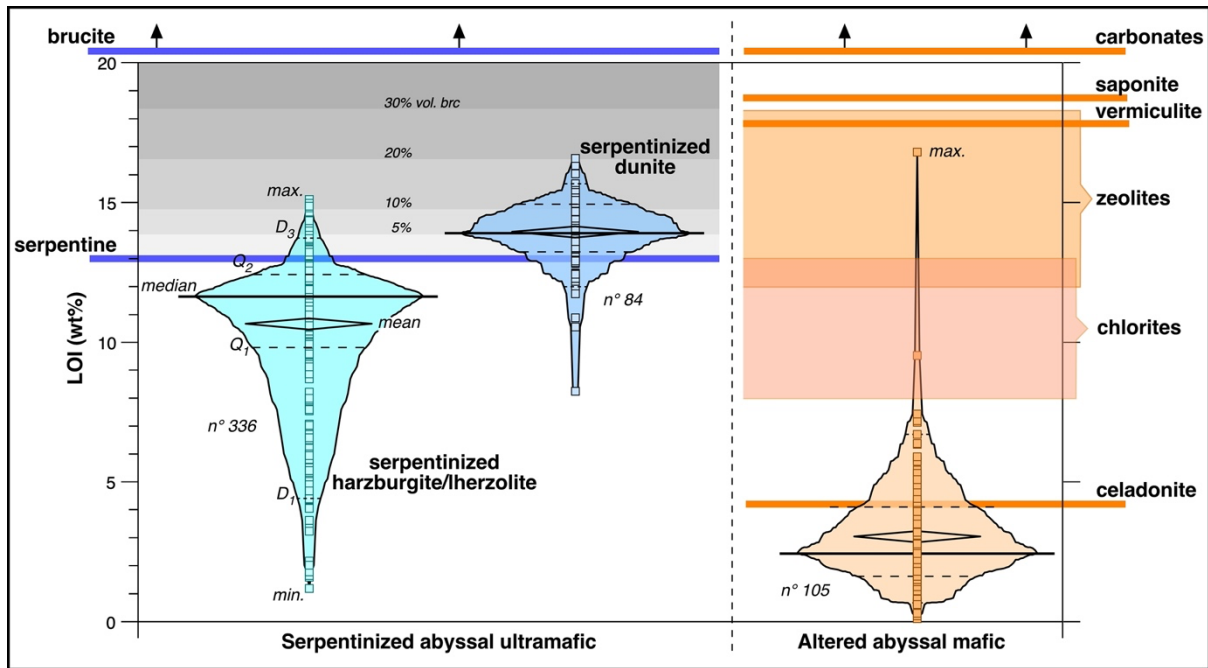
314 **Figures and captions**



315

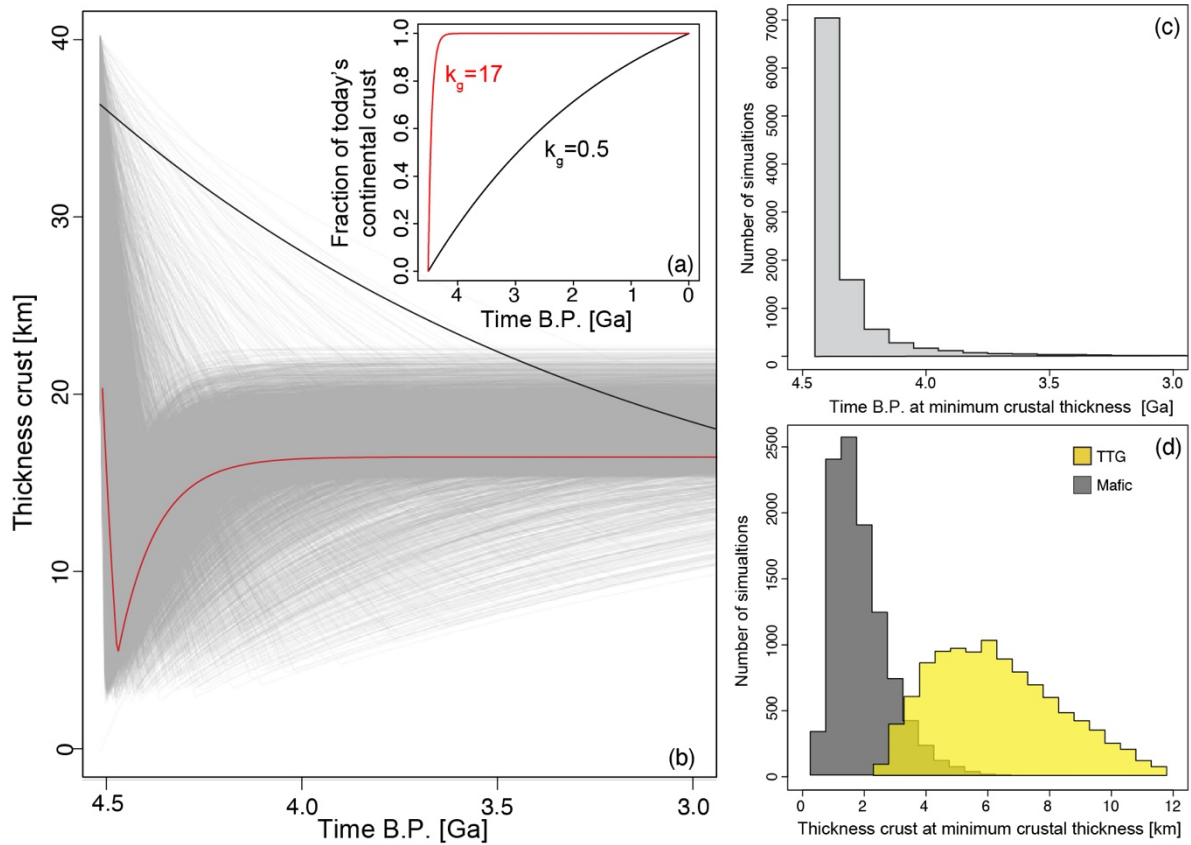
316 **Figure 1: An idealised sketch of one of the hydrothermal systems that constituted the**
 317 **global hydrothermal reactor in the Hadean-Archean.** The sketch is based on samples and
 318 geological evidence collected at the Lost City Hydrothermal Field. The widespread availability
 319 of seawater-mantle interfaces in the early Earth triggered the diffusion of brucite in a large
 320 variety of environments (subterranean, submarine and even subaerial) dominated by alkaline,
 321 reduced conditions. The residual character of Hadean mantle rocks maximised the diffusion of
 322 brucite, with its unique catalytic properties, providing an unrepeatabeable global scenario for
 323 prebiotic synthesis. Lost City image courtesy of D. Kelley and M. Elend (University of
 324 Washington).

325



326

327 **Figure 2:** Box-percentile plots for abyssal serpentinized upper mantle rocks and altered basalts
328 showing a distinct degree of alteration (visualised by loss on ignition; LOI). Mean and median
329 of serpentinite LOI roughly overlap the LOI of serpentine minerals (with a variable brucite
330 content) indicating the extreme efficiency of the hydration process. On the contrary, the mean
331 and the median of altered basalt LOI are much lower than the LOI of the alteration assemblage
332 (smectites, chlorites, zeolites and celadonite) indicating a less efficient reaction process.
333 Furthermore, box-percentile plots for serpentinized lherzolite-harzburgite and dunites indicate
334 that olivine-dominated systems, characteristic of the residual Hadean-Archean mantle, produce
335 larger amounts of brucite. Data collected from Refs.^{30,32,34,35,55}.



336

337

338 **Figure 3: Results of the mass balance calculations.** a) End members model for the evolution

339 of the mass of the continental crust in time. In the Monte Carlo simulations we randomly

340 sample between the two end member model shown by the red and black curve. b) Grey lines

341 show the evolution of the crust thickness (Hadean ,continental and mafic produced by partial

342 melting of the mantle; Methods) in time. The black and red line are for two simulations

343 considering the two end-member growth scenarios presented in panel a. c) Distribution of times

344 at which the thickness of the crust reaches minimum values. c) distributions of the thickness of

345 mafic and TTG-type crust once the total crustal thickness is at its minimum.